

# New Criterion for Evaluating the Peak Shear Strength of Rock Joints Under Different Contact States

Zhi Cheng Tang<sup>1,2</sup> · Louis Ngai Yuen Wong<sup>3,4</sup>

Received: 6 February 2015 / Accepted: 1 August 2015 / Published online: 14 August 2015  
© Springer-Verlag Wien 2015

**Abstract** In practice, the peak shear strength of rock joints is not dictated only by the surface roughness, but also the degree of matching between the joint surfaces. The latter is due to alteration/dislocation caused by external factors, such as the vibration due to nearby blasting, excavation or earthquake. In the present study, the peak shear strengths of rock joints under different contact states are investigated by direct shear test using artificial rock joints. The rock joints under different contact states are modeled by imposing varying magnitude of horizontal dislocation along the shear direction between the upper and lower rock blocks. The peak shear strength was found to decrease with increasing dislocation. A new empirical shear strength criterion is put forward to capture the peak shear strength of un-matching rock joints as an extension of a previously published peak shear strength criterion for matching rock joints by the first author and his co-workers. In the present proposed criterion, a new joint contact state coefficient, which is a function of the normalized

dislocation and the quantified three-dimensional roughness metric of joint surface, is proposed. The good agreement between calculated values and test results indicates that the proposed criterion is capable of estimating the peak shear strength of rock joints under different contact states. The proposed criterion is expressed in a quantitative way and the required parameters can be easily determined in the laboratory.

**Keywords** Rock joint · Peak shear strength criterion · Contact state · Joint contact state coefficient (JCC) · Quantified three-dimensional roughness metric · Normalized dislocation

## List of symbols

$A_0$	Normalized area corresponding to apparent dip angle $\theta_{\max}^* = 0$
$C$	Roughness parameter characterizing distribution of apparent dip angles over joint surface
$d$	Imposed dislocation between the upper and lower rock blocks (mm)
$E$	Young's modulus (GPa)
$i$	Positive integer
JCC	Joint contact state coefficient
JCS	Joint wall compressive strength (MPa)
JMC	Joint matching coefficient
JRC	Joint roughness coefficient
$l$	Length of rock joint along the shear direction (mm)
$m$	The number of test results
$\theta_{\max}^*$	Maximum apparent dip angle in the shear direction (°)
$\beta$	Angle between schistosity plane and plane normal to the joint (°)
$\varphi_b$	Basic friction angle of rock joint (°)

L. N. Y. Wong was formerly at School of Civil and Environmental Engineering, Nanyang Technological University.

✉ Louis Ngai Yuen Wong  
lnywong@ntu.edu.sg

<sup>1</sup> School of Civil and Architectural Engineering, Wuhan University, Wuhan 430072, People's Republic of China

<sup>2</sup> School of Civil and Environmental Engineering, Nanyang Technological University, Block N1, Nanyang Avenue, 639798 Singapore, Singapore

<sup>3</sup> Department of Earth Sciences, The University of Hong Kong, Hong Kong, People's Republic of China

<sup>4</sup> School of Mechanics and Civil Engineering, China University of Mining and Technology, 1 Daxue Road, Xuzhou 221116, Jiangsu, People's Republic of China

$\varphi_r$	Residual friction angle ( $^\circ$ )
$\tau$	Shear strength of smooth joint (MPa)
$\tau_p$	Peak shear strength of rough joint (MPa)
$\tau_{p\_cal}$	Calculated peak shear strength by criterion (MPa)
$\tau_{p\_mea}$	Measured peak shear strength (MPa)
$\delta_{peak}$	Peak shear displacement (mm)
$e_{ave}$	Average estimated error
$\sigma_c$	Compressive strength of model material (MPa)
$\sigma_n$	Normal stress (MPa)
$\sigma_t$	Tensile strength of model material (MPa)
$\kappa$	Ratio of imposed dislocation to the length of sample along shear direction, $d/l$
$\nu$	Poisson's ratio
$\rho$	Density ( $\text{kg/m}^3$ )

## 1 Introduction

Natural rock masses usually contain cracks and joints which have a great influence on the deformation and shear behavior of rock masses. The mobilization of shear strength of rock joints that become potential failure planes is significant to a variety of rock engineering applications, e.g., slope stability of hard rock masses, and roof and sidewall stability of underground excavation. An accurate determination of the shear strength of rock joints is critical as small changes of such can result in significant changes in the safety of structures, both in and on rock masses (Zhao 1997a). Performing direct shear tests on small-scale specimens in laboratory is a prerequisite to comprehensively understand the large-scale behavior of rock joints in situ. The shear behavior of rock joints is influenced by many factors, such as morphology, normal stress, compressive or tensile strength of joint material, surface matching, boundary conditions during the process of shearing, scale effect, shear rate and asperity deformability. Patton (1966) firstly stated the importance of the shape of surface profile to the shear strength of rock joints. Several shear failure criteria incorporating morphology parameters have been developed (Barton 1973; Barton and Choubey 1977; Kulatilake et al. 1995; Zhao 1997a; Homand et al. 2001; Grasselli 2006; Xia et al. 2014). Among these, the JRC-JCS criterion developed by Barton and Choubey (1977) has been the most widely used due to its simplicity. Although JRC determination is subject to a certain degree of subjectivity with regard to the roughness characterization, other more sophisticated methods (based on various techniques including fractal-based approaches, laser scanner, or photogrammetry, etc.) have not yet gained a widespread popularity among the practicing engineers. Nonetheless, a number of peak shear strength criteria based on these more

advanced techniques of roughness assessment have been developed, among which we can highlight those of Kulatilake et al. (1995), Grasselli (2006) and Xia et al. (2014).

Most of the previous research focused on the shear behavior of matching rock joints. However, the contact between two blocks with irregular morphology can be subjected to alteration during its course of history, such as the vibration caused by nearby blasting, excavation or earthquake. Hence, the matching joint will become un-matching and the corresponding shear strength will be different. Zhao (1997a, b) defined a roughness-independent geometrical parameter JMC (joint matching coefficient) to describe this alteration and proposed a modified version of JRC-JCS criterion with the inclusion of JMC, namely the JRC-JMC criterion. Oh and Kim (2010) later investigated the effect of opening on the shear behavior of regularly shaped rock joint by imposing some dislocation between the two contact blocks. Although a better understanding of the shear behavior of rock joint has been obtained, the above two modified JRC-based criteria did not practically address and overcome the inherent limitations associated with JRC (Beer et al. 2002; Hong et al. 2008). As for the JRC-JMC criterion, how to realistically determine JMC is still a challenging open question.

In the present research, replicas of matching natural rock joint with different morphology were prepared by using three different model materials. The un-matching joints were then modeled by imposing varying magnitude of horizontal dislocation between the two blocks. An empirical criterion for estimating the peak shear strength of rock joint was subsequently proposed based on a large number of direct shear test results. Although the imposed dislocations on the matching joints in the present study may not realistically represent the un-matching rock joints in the field, the present results provide the essential fundamentals for evaluating the shear behavior of un-matching rock joints in the laboratory.

## 2 Sample Preparation

To investigate the effect of contact state on the peak shear strength of rock joints, it is necessary to perform direct shear tests on samples having identical geometrical features. However, it is practically impossible to find two different natural rock joints with the same morphology. Therefore, replicas of rock joints were used in the present study. A number of rock joints were obtained by splitting granite blocks using the Brazilian tensile testing method, which were obtained from Quanzhou (stone material supply base), Fujian province, China. Five rough surfaces were selected as parent model. To obtain matching replicas of

**Table 1** Main features of the experimental model materials

Group	Plaster:sand:water (weight ratio)	Joint	Length × width (mm × mm)	Curing conditions	Mechanical properties					
					$\sigma_c$ (MPa)	$\sigma_t$ (MPa)	$\phi_b$ (°)	$\rho$ (kg/m <sup>3</sup> )	$E$ (GPa)	$\nu$
A	3: 2:1	J-I	300 × 150	Temperature = 25 °C Humidity = 90 % Days = 28	27.5	1.54	35	2200	6.1	0.16
		J-II								
		J-III								
B	3: 3:2	J-IV <sup>+</sup>	200 × 100	Temperature = 25 °C Humidity = 90 % Days = 28	16.1	1.37	31	2010	4.3	–
		J-IV <sup>-</sup>								
		J-V <sup>+</sup>								
		J-V <sup>-</sup>								
C	1: 0:1	J-IV <sup>+</sup>	200 × 100	Temperature = 25 °C Humidity = 90 % Days = 20	4.7	0.64	24.8	1750	1.9	–
		J-V <sup>+</sup>								

<sup>+</sup> Forward direction; <sup>-</sup> reverse direction

natural rock joints, silicone rubber was used to capture the topographic features of natural rock joints. Either the upper surface or the lower surface of each joint was firstly molded by using a mixture of plaster, sand and water. Table 1 provides the model mixtures, dimensions, curing conditions and the related mechanical parameters of the model materials. Three groups of specimens, namely Groups A, B and C, were prepared according to the used artificial model material.

A three-dimensional stereo-topometric measurement system was used for the joint roughness measurements. The quantified three-dimensional roughness metric developed by Tatone and Grasselli (2009) was used to characterize the surface morphology. The surface feature along the shear direction can be captured by  $A_0$ ,  $\theta_{max}^*$  and  $C$ . The values of these quantified morphology parameters of the joints are listed in Table 2. Roughness profiles were obtained in the shear direction along nine equally spaced straight lines on the model joint surface. Along each line the surface height was recorded at every 0.3 mm, at an accuracy of up to 0.02 mm. JRC values were visually determined by three experienced rock mechanics researchers by comparing the selected profiles against the

ten standard profiles proposed by Barton and Choubey (1977) and suggested by ISRM (1978). The results are listed in Table 2.

By imposing varying lateral dislocation between the upper and lower rock blocks along the shear direction, we can obtain a series of un-matching joints with a morphology identical to that of the matching one. For Group A, the lateral dislocation was set to be 0, 5, 10, or 15 mm, respectively; for Groups B and C, the lateral dislocation was set to be 0, 2, 4, or 8 mm, respectively. Zero dislocation represents the matching joint. Special attention was paid to the process of imposing dislocation on the upper and lower rock blocks to avoid the damage of asperities, especially for the soft-material (Group C). In the present study, the parameter  $\kappa$  is used to describe the ratio of imposed dislocation ( $d$ ) to the length of sample along the shear direction ( $l$ ). The procedures of imposing lateral dislocation between the upper and lower blocks of rock joint are described below (Tang et al. 2014):

- The upper and lower blocks are placed tightly together to form a closed joint.

**Table 2** The morphology parameters of the test joints

Morphology	JRC by visual comparison				$A_0$	$\theta_{max}^*$ (°)	$C$
	Mean	Standard deviation	Maximum	Minimum			
J-I	6.3	1.70	12–14	2–4	0.499	59.0	10.5
J-II	12.8	2.01	18–20	6–8	0.504	69.3	8.01
J-III	17.1	1.34	18–20	12–14	0.688	68.7	7.48
J-IV <sup>+</sup>	3.7	0.81	4–6	2–4	0.513	44.7	9.27
J-IV <sup>-</sup>	3.3	0.73	4–6	2–4	0.501	43.9	9.82
J-V <sup>+</sup>	14.1	1.14	16–18	10–12	0.534	78.4	9.05
J-V <sup>-</sup>	13.6	1.26	16–18	8–10	0.506	75.6	9.38

<sup>+</sup> Forward direction; <sup>-</sup> reverse direction

- Under this completely matching condition, a set of parallel vertical scale lines are drawn at 1.0-mm intervals across the two surfaces of the joint plane.
- The lower block is held fixed.
- The upper block is then lifted up several centimeters and moved slowly to make a lateral dislocation  $d$ , with reference to the scale lines. During the movement, there is no contact between the two blocks until the block arrives at the target position.
- The upper block is placed without rotation by using a horizontal positioning device.

### 3 Test Procedures and Results

In the present study, direct shear test experiments were conducted on artificial rock joints under constant normal load (CNL) condition using servo-hydraulic direct shear test equipment. The apparatus consists of steel shear boxes, 300 mm in length, 150 mm in width and 150 mm in height, respectively. During the course of testing, all data (normal force, shear force, horizontal displacement and vertical displacement) were monitored and recorded by a data acquisition system connected to a computer. The shear displacement was measured by two LVDTs with an accuracy of 0.1 mm and the data recording rate was 100 data points per second. The normal loads of 0.5, 1.0, 1.5, 2.0 and 3.0 MPa were applied for Group A, 0.4, 0.8, 1.2, 1.6 and 2.0 MPa for Group B and 0.2, 0.4, 0.6 0.8 and 1.0 MPa for Group C, respectively. The shear velocity was set to be 0.5 mm/min for all tests. Each test was performed on a

“new” joint and no specimen was used repeatedly. Refer to Tang (2013) and Xia et al. (2014) for the detailed test procedures.

Generally, the upper block will rotate a small angle due to the rough nature of the two surfaces and the contact between the two blocks becomes unstable after imposing a lateral dislocation. To eliminate the effect of rotation on the shear behavior of rock joints, two pairs of balance fixture were used to place the upper block in a horizontal level when it was moved to the target position. The device was removed after the normal stress had been applied to the pre-selected target value. The upper block was not allowed to rotate before applying the shear loading.

In order to ascertain the reproducibility of tests results, Group A was selected and repeated three times for matching joints; three tests were randomly selected and repeated three times for un-matching joints for each contact state in the three groups, respectively. The maximum difference between the shear strength of each pair of the tests was 2.84 % for matching joints and 4.32 % for un-matching joints.

Samples with varying dislocation were subjected to direct shear tests at various normal stress levels. Tables 3, 4 and 5 list the peak shear strength ( $\tau_p$ ) and the corresponding peak shear displacement ( $\delta_{peak}$ ). The results show that the peak shear strength of rock joints decreases with increasing dislocation and the trend of peak shear strength of rock joints under different contact state is shown in Fig. 1 (taken J-I as an example). As normal stress increases, the effect of dislocation becomes less pronounced.

**Table 3** Peak shear strength and corresponding peak shear displacement for Group A (Tang 2013)

Joint	$\sigma_n$	$\tau_p$ at following dislocation				$\delta_{peak}$ at following dislocation				$\tau$ for smooth joint calculated by friction law ( $\tau = \sigma_n \tan \phi_b$ )
		0 mm	5 mm	10 mm	15 mm	0 mm	5 mm	10 mm	15 mm	
J-I	0.5	0.85	0.67	0.55	0.43	4.87	3.43	3.01	4.15	0.35
	1.0	1.19	1.03	0.88	0.71	3.54	4.08	3.39	3.87	0.70
	1.5	1.77	1.51	1.32	1.19	2.88	2.59	3.14	3.22	1.05
	2.0	2.24	2.00	1.74	1.52	1.08	2.00	3.26	2.99	1.40
	3.0	2.84	2.52	2.33	2.12	0.97	2.32	2.14	3.31	2.10
J-II	0.5	1.13	0.93	0.73	0.50	3.35	3.07	3.99	4.72	0.35
	1.0	1.75	1.25	1.00	0.75	2.46	2.88	3.02	3.64	0.70
	1.5	2.20	1.70	1.24	1.23	2.89	3.11	3.87	3.51	1.05
	2.0	2.78	2.11	1.78	1.55	2.07	3.08	4.32	3.74	1.40
	3.0	3.34	2.70	2.50	2.20	1.49	3.08	2.69	3.66	2.10
J-III	0.5	1.78	1.18	1.01	0.88	3.67	3.44	2.91	3.33	0.35
	1.0	2.42	1.89	1.80	1.67	2.51	3.05	3.74	4.36	0.70
	1.5	2.89	2.66	2.39	2.12	3.08	3.27	3.29	4.01	1.05
	2.0	3.51	2.91	2.68	2.27	3.24	2.66	3.88	4.29	1.40
	3.0	4.20	3.61	3.38	3.15	2.91	2.53	3.94	3.55	2.10

**Table 4** Peak shear strength and corresponding peak shear displacement for Group B

Joint	$\sigma_n$	$\tau_p$ at following dislocation				$\delta_{peak}$ at following dislocation				$\tau$ for smooth joint calculated by friction law ( $\tau = \sigma_n \tan \phi_b$ )
		0 mm	2 mm	4 mm	8 mm	0 mm	2 mm	4 mm	8 mm	
J-IV <sup>+,B</sup>	0.40	0.418	0.326	0.289	0.268	3.87	3.08	4.25	4.00	0.240
	0.80	0.793	0.708	0.655	0.503	4.02	5.06	3.88	3.89	0.481
	1.20	1.106	0.967	0.912	0.827	2.69	3.07	4.41	4.50	0.721
	1.60	1.442	1.257	1.033	0.970	2.78	3.33	4.29	4.05	0.961
	2.00	1.709	1.554	1.387	1.241	1.84	1.97	2.26	3.87	1.202
J-IV <sup>-,B</sup>	0.40	0.391	0.328	0.267	0.248	3.54	4.11	4.08	5.27	0.240
	0.80	0.726	0.637	0.557	0.511	3.29	3.03	3.88	4.67	0.481
	1.20	1.117	0.903	0.842	0.764	2.83	3.25	3.67	4.08	0.721
	1.60	1.406	1.207	1.006	0.965	3.44	3.07	3.57	3.87	0.961
	2.00	1.669	1.449	1.362	1.229	2.71	2.84	4.07	4.11	1.202
J-V <sup>+,B</sup>	0.40	0.601	0.441	0.325	0.276	4.37	3.89	4.24	4.17	0.240
	0.80	0.984	0.771	0.634	0.506	4.08	4.85	4.56	5.07	0.481
	1.20	1.483	1.187	0.864	0.801	3.88	4.22	4.67	4.43	0.721
	1.60	1.857	1.445	1.285	1.156	3.97	4.02	4.14	4.69	0.961
	2.00	2.230	1.893	1.653	1.435	3.61	3.54	3.99	4.27	1.202
J-V <sup>-,B</sup>	0.40	0.552	0.467	0.421	0.394	4.13	3.74	4.36	4.57	0.240
	0.80	0.934	0.726	0.653	0.600	4.07	4.33	4.29	4.91	0.481
	1.20	1.367	1.007	0.896	0.825	3.57	4.01	4.24	5.07	0.721
	1.60	1.706	1.442	1.139	1.004	3.66	3.84	4.06	4.67	0.961
	2.00	2.008	1.773	1.525	1.366	3.19	3.77	4.29	4.58	1.202

<sup>+</sup> Forward direction; <sup>-</sup> reverse direction

<sup>B</sup> Group B

**Table 5** Peak shear strength and corresponding peak shear displacement for Group C

Joint	$\sigma_n$	$\tau_p$ at following dislocation				$\delta_p$ at following dislocation				$\tau$ for smooth joint calculated by friction law ( $\tau = \sigma_n \tan \phi_b$ )
		0 mm	2 mm	4 mm	8 mm	0 mm	2 mm	4 mm	8 mm	
J-IV <sup>+,C</sup>	0.20	0.154	0.123	0.101	0.093	4.10	4.38	4.91	5.55	0.089
	0.40	0.288	0.226	0.193	0.185	3.48	4.07	4.21	5.08	0.179
	0.60	0.442	0.374	0.322	0.284	2.94	4.33	4.67	5.08	0.268
	0.80	0.568	0.483	0.422	0.374	3.07	3.77	3.64	4.02	0.358
	1.00	0.703	0.588	0.526	0.497	3.01	3.35	4.2	4.07	0.477
J-V <sup>+,C</sup>	0.20	0.215	0.187	0.143	0.122	3.94	4.66	4.91	5.67	0.089
	0.40	0.400	0.324	0.287	0.223	3.65	3.94	4.67	4.93	0.179
	0.60	0.562	0.487	0.433	0.400	3.27	4.06	4.22	4.68	0.268
	0.80	0.687	0.537	0.467	0.443	3.66	3.72	4.08	4.29	0.358
	1.00	0.843	0.728	0.653	0.627	4.12	3.46	3.86	4.77	0.477

<sup>+</sup> Forward direction

<sup>C</sup> Group C

## 4 Peak Shear Strength Criterion

### 4.1 Previous Study

A new peak shear strength criterion, Eq. (1), was recently developed by the first author and his co-workers to capture

the peak shear strength of matching rock joints (Xia et al. 2014). Here, further published direct shear test results (listed in Table 6) and the present results were compiled and analyzed to verify the criterion. The comparison between the test results and the calculated values is plotted in Fig. 2. The average estimated error calculated by Eq. (2)

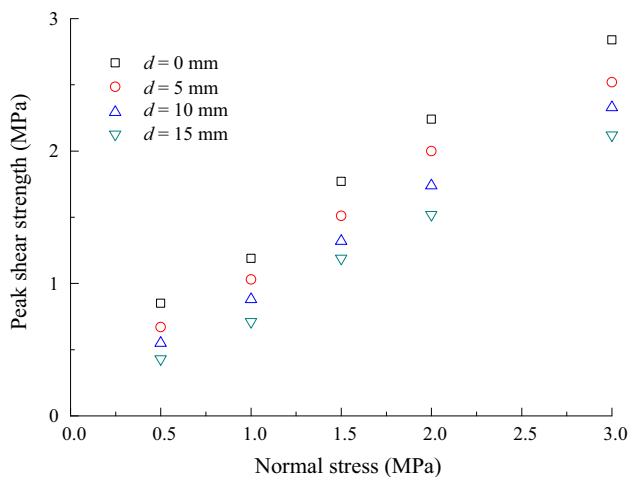


**Fig. 1** Peak shear strength of rock joint under different contact state (J-I)

for the value predicted by the criterion was 11.91 % for the 102 data points. As such, the criterion can be considered generally applicable to predict the peak shear strength of matching rock joints with an acceptable accuracy. This provides the basis for the following analysis.

$$\tau_p = \sigma_n \tan \left\{ \varphi_b + 4 \frac{A_0 \theta_{max}^*}{1+C} \left[ 1 + \exp \left( -\frac{1}{9A_0} \cdot \frac{\theta_{max}^*}{1+C} \cdot \frac{\sigma_n}{\sigma_t} \right) \right] \right\} \tag{1}$$

$$e_{ave} = \frac{1}{m} \sum_{i=1}^m \left| \frac{\tau_{p\_mea} - \tau_{p\_cal}}{\tau_{p\_mea}} \right| \times 100 \% \tag{2}$$

### 4.2 New Failure Criterion

Equation (1) cannot be readily used to evaluate the peak shear strength of un-matching rock joints. If the effect of matching condition is ignored, the correlation coefficient between the peak shear strength of rock joints directly calculated by Eq. (1) and the test results would decrease drastically. To develop a new empirical criterion to capture the peak shear strength of rock joints with different degree of matching, a general function based on Eq. (1) and with reference to the mathematical expression of JRC-JMC criterion proposed by Zhao (1997a) was proposed, which was given as:

$$\tau_p = \sigma_n \tan \left\{ \varphi_b + f \left( \frac{A_0 \theta_{max}^*}{1+C}, \kappa \right) \cdot 4 \frac{A_0 \theta_{max}^*}{1+C} \times \left[ 1 + \exp \left( -\frac{1}{9A_0} \cdot \frac{\theta_{max}^*}{1+C} \cdot \frac{\sigma_n}{\sigma_t} \right) \right] \right\}, \tag{3}$$

where  $f(\dots)$  is a suitably chosen function that accounts for the influence of mismatch on shear strength of rock joints.

To determine the specific form of  $f\left(\frac{A_0 \theta_{max}^*}{1+C}, \kappa\right)$ , the raw data set was subjected to least squares regression analysis by using Eq. (3). Several simple combinations of  $\frac{A_0 \theta_{max}^*}{1+C}$  and  $\kappa$  were used to perform regression analysis. Linear, power, logarithmic, exponential and hyperbolic curve-fitting approximations were executed and the approximation equation was determined by minimization of the sum of squared errors. Another exercised principle was to minimize the number of fitting coefficients. Finally, a simple hyperbolic function was selected and the specific formula of Eq. (3) was given as Eq. (4). The correlation between the calculated values and the test results is shown in Fig. 3.

$$\tau_p = \sigma_n \tan \left\{ \varphi_b + \left[ \frac{1}{1 + 8A_0 \theta_{max}^* / (1+C)} \cdot \kappa \right] \cdot \frac{4A_0 \theta_{max}^*}{1+C} \times \left[ 1 + \exp \left( \frac{1}{9A_0} \cdot \frac{\theta_{max}^*}{1+C} \cdot \frac{\sigma_n}{\sigma_t} \right) \right] \right\} \tag{4}$$

According to the present study, the peak shear strength is influenced by both the roughness and the contact state. The particular form chosen for  $f(\dots)$  is called “joint contact state coefficient” (JCC):

$$JCC = \frac{1}{1 + \frac{8A_0 \theta_{max}^*}{(1+C)} \times \frac{d}{l}} \tag{5}$$

Referring to Eq. (1), the peak dilatancy angle is  $\frac{8A_0 \theta_{max}^*}{(1+C)}$  as  $\sigma_n \rightarrow 0$ , which is called the initial peak dilatancy angle and determined by the quantified three-dimensional roughness metric (Xia et al. 2014). Thus, JCC is a function of the initial dilatancy angle and the normalized dislocation. It should be pointed that the coefficient “8” on the right-hand side of Eq. (5) is not obtained based on the best fitting result. As shown in Fig. 4, the sum of squared errors would be minimized as the fitting-coefficient approaches 6.6 (the sum of squared errors is 9.126). Considering the small discrepancy of the sum of squared error for 6.6 and 8 (9.126 versus 9.267), we finally take 8 as the coefficient.

As such, the undetermined function,  $f\left(\frac{A_0 \theta_{max}^*}{1+C}, \kappa\right)$ , can be determined in a quantitative way as a function of quantified three-dimensional roughness metric and normalized dislocation. Thus, we can say that there is no fitting coefficient for the parameter JCC. A similar treatment was also performed by other researchers, such as Barton (1973), to obtain a simple expression of the peak dilatancy angle involving a small rotation from the best line in the original version of JRC-JCS criterion.

The influence of the quantified three-dimensional roughness metric and the normalized dislocation on JCC is shown in Fig. 5. For a smooth joint, JCC remains at the maximum value and it is not affected by the dislocation. For a rough joint, the degree of matching is expected to

**Table 6** Experimental data of matching rock joints

Sample name	Rock type	$\beta$ (°)	$A_0$	$C$	$\theta_{\max}^*$ (°)	$\sigma_n$ (MPa)	$\sigma_n/\sigma_t$	$\varphi_b$ (°)	$\varphi_r$ (°)	Peak shear strength (MPa)
C1	Limestone	–	0.491	7.03	80	1.07	0.45	36	60	2.2
C2	Limestone	–	0.462	5.64	80	1.07	0.45	36	56	2.1
C3	Limestone	–	0.46	4.6	57	3.72	1.55	36	51	5.5
C4	Limestone	–	0.508	4.74	65	2.45	1.02	36	53	4.6
C5	Limestone	–	0.495	5.26	74	3.11	1.30	36	53	5.0
C6	Limestone	–	0.546	5.19	68	1.02	0.43	36	59	2.1
C8	Limestone	–	0.555	5.71	74	3.11	1.30	36	53	4.9
G1	Granite	–	0.493	7.17	90	2.3	0.26	34	51	5.7
G2	Granite	–	0.498	5.6	80	2.3	0.26	34	53	5.6
G4	Granite	–	0.498	5.48	65	2.19	0.25	34	52	4.8
G5	Granite	–	0.46	5.33	57	1.12	0.13	34	54	2.4
G6	Granite	–	0.477	7.39	84	1.12	0.13	34	57	2.9
G7	Granite	–	0.47	7.15	81	1.12	0.13	34	57	2.8
G9	Granite	–	0.508	5.85	75	1.12	0.13	34	57	3.0
M1	Marble	–	0.513	9.64	76	0.87	0.09	37	54	1.7
M2	Marble	–	0.492	5.6	39	1.73	0.19	37	46	2.3
M3	Marble	–	0.471	10.5	65	0.87	0.09	37	52	1.2
M4	Marble	–	0.513	8.12	61	3.78	0.41	37	47	5.8
M5	Marble	–	0.533	8.92	59	2.6	0.28	37	49	4.4
M6	Marble	–	0.45	10.18	68	2.6	0.28	37	48	4.3
M7	Marble	–	0.502	13.33	86	3.78	0.41	37	46	5.6
M8	Marble	–	0.459	10.52	72	3.83	0.42	37	48	6.4
M9	Marble	–	0.494	10.36	59	2.6	0.28	37	47	4.5
M10	Marble	–	0.515	10.79	67	0.87	0.09	37	57	1.5
M12	Marble	–	0.429	7.28	55.0	1.79	0.20	37	58	3.0
ML1	Sandstone	–	0.573	7.25	66	1.02	1.46	37	51	1.4
ML2	Sandstone	–	0.505	5.44	45	4.13	5.90	37	43	4.5
ML3	Sandstone	–	0.523	7.81	66	2.09	2.99	37	45	2.3
Gn3	Gneiss	90	0.492	8.11	65	2.65	0.28	36	38	2.4
Gn6	Gneiss	0	0.522	4.91	63	1.90	0.54	36	46	3.4
Gn9	Gneiss	90	0.488	8.12	63	3.52	0.37	36	37	4.0
Gn10	Gneiss	90	0.500	8.18	70	3.57	0.38	36	40	3.9
Gn11	Gneiss	90	0.432	10.28	74	3.52	0.37	36	37	4.3
Gn12	Gneiss	90	0.506	11.12	85	4.08	0.43	36	35	3.3
Gn13	Gneiss	90	0.503	9.17	74	2.60	0.27	36	36	3.5
S1	Serpentinite	0	0.504	4.80	79	1.94	0.32	39	53	4.3
S2	Serpentinite	0	0.466	4.44	75	0.97	0.16	39	61	3.4
Gr-1	Granite	–	0.610	10.26	79.67	0.8	0.090	34	–	1.5
Gr-2	Granite	–	0.530	9.85	81.76	1.6	0.180	34	–	3.1
Gr-3	Granite	–	0.480	10.08	83.63	2.4	0.270	34	–	4.8
Gr-4	Granite	–	0.510	9.28	82.06	3.2	0.360	34	–	5.8
Gr-5	Granite	–	0.470	10.41	79.32	4.0	0.450	34	–	6.4
Gr-6	Granite	–	0.490	10.28	81.58	4.8	0.540	34	–	7.3
Gr-7	Granite	–	0.530	11.17	81.06	5.6	0.630	34	–	8.5
Gr-8	Granite	–	0.560	9.56	84.05	6.4	0.720	34	–	11.0
Gr-9	Granite	–	0.510	9.61	82.59	7.2	0.810	34	–	11.2
Gr-10	Granite	–	0.530	8.30	82.23	8.0	0.900	34	–	12.7
Sa-1	Sandstone	–	0.510	8.85	83.32	0.325	0.125	28	–	0.7

**Table 6** continued

Sample name	Rock type	$\beta$ ( $^{\circ}$ )	$A_0$	$C$	$\theta_{\max}^{\circ}$ ( $^{\circ}$ )	$\sigma_n$ (MPa)	$\sigma_n/\sigma_t$	$\varphi_b$ ( $^{\circ}$ )	$\varphi_r$ ( $^{\circ}$ )	Peak shear strength (MPa)
Sa-2	Sandstone	–	0.610	7.61	82.27	0.650	0.250	28	–	0.9
Sa-3	Sandstone	–	0.540	8.39	82.60	0.975	0.375	28	–	1.5
Sa-4	Sandstone	–	0.490	8.92	83.85	1.300	0.500	28	–	2.0
Sa-5	Sandstone	–	0.550	9.52	82.72	1.625	0.625	28	–	2.1
Sa-6	Sandstone	–	0.580	7.92	81.62	1.950	0.750	28	–	3.0
Sa-7	Sandstone	–	0.500	8.93	82.86	2.275	0.875	28	–	3.3
Sa-8	Sandstone	–	0.470	8.84	83.53	2.600	1.000	28	–	3.6
Sa-9	Sandstone	–	0.440	9.27	83.35	2.925	1.125	28	–	3.8
Sa-10	Sandstone	–	0.510	8.34	84.21	3.250	1.250	28	–	4.7

C1, C2, ..., S1, S2: Grasselli (2006); Gr-1, Gr-2, ..., Sa-9, Sa-10: Yang et al. (2015)

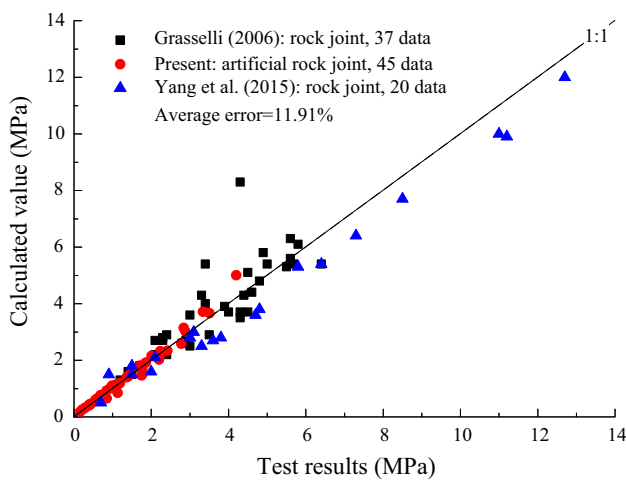


**Fig. 2** Comparison between measured and calculated peak shear strength for matching joints

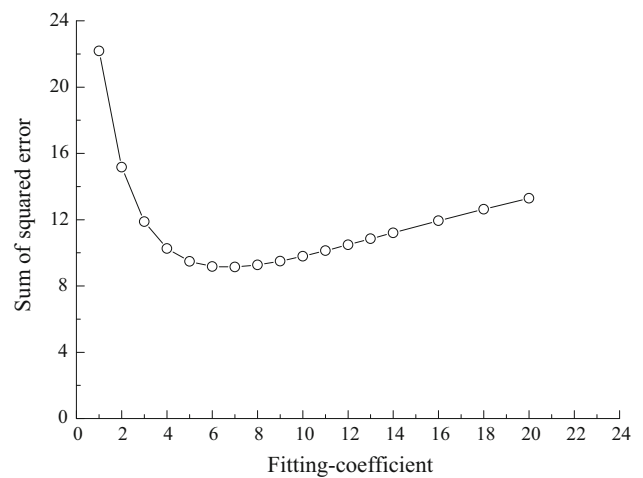


**Fig. 4** Relationship between the fitting-coefficient and the sum of squared error

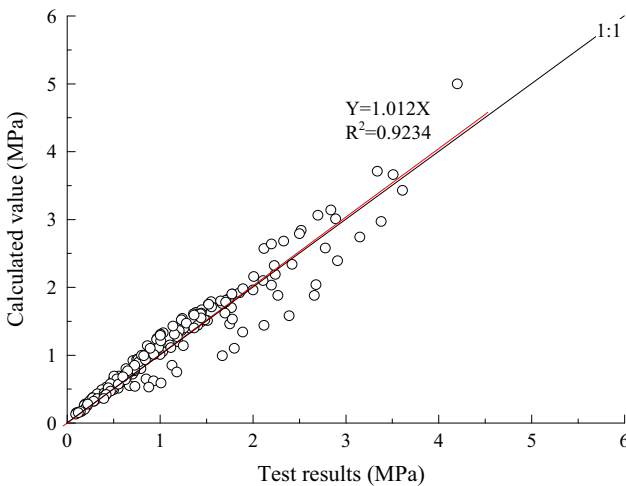


**Fig. 3** Peak shear strength calculated by Eq. (4) versus the test results

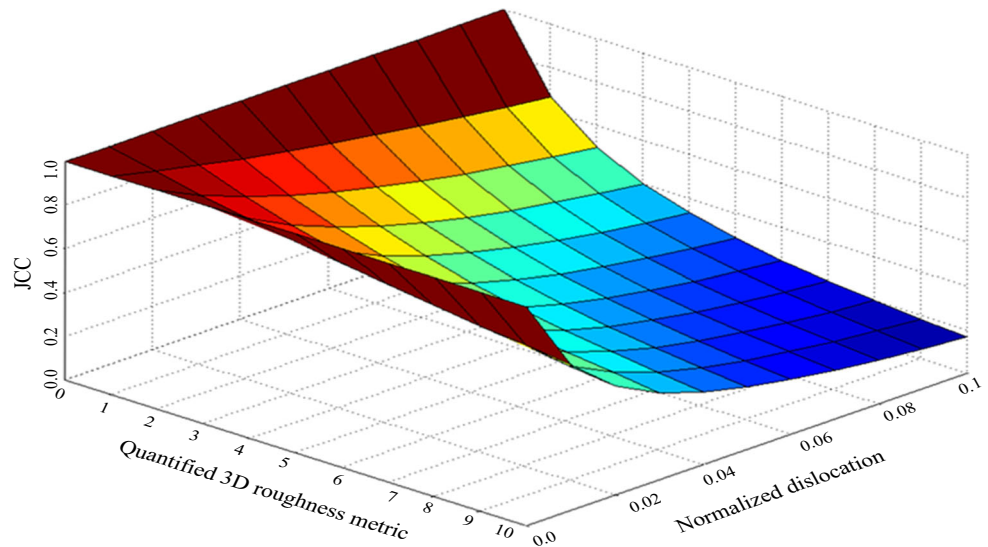
decrease rapidly from its initial matching state at the beginning. As shown in Fig. 5, JCC decreases at a higher rate at the initial state and the rate decreases with increasing dislocation. After some distance of dislocation, JCC is expected to approach the minimum value. In the present study, the value of the normalized dislocation  $\kappa$  is no more than 0.05 ( $\kappa \leq 0.05$ ).

### 5 Conclusions

Models available in the literature for evaluating the peak shear strength of rock joints typically neglected the combined effects of three-dimensional roughness and joint matching condition. By imposing varying magnitudes of dislocation between upper and lower rock blocks to obtain a series of un-matching joints with different degree of matching, a large number of direct shear tests have been



**Fig. 5** Influence of quantified 3D roughness metric and normalized dislocation on JCC



performed. The peak shear strength was found to decrease with increasing dislocation and as the normal stress increases, the effect of dislocation becomes less pronounced. An empirical peak shear strength criterion was proposed with the inclusion of the normalized dislocation to estimate the peak shear strength of rock joint with different degree of matching. A new joint contact state coefficient (JCC), which is expressed as a function of quantified three-dimensional roughness metric and normalized dislocation, was introduced. Since the proposed criterion was developed based on empirical analysis, more experiments should be conducted to further validate the criterion in future research.

**Acknowledgments** The authors gratefully acknowledge the support from the Natural Science Foundation of China under project 41402247, the National Basic Research Program of China (973 Program) under project 2014CB046904 and the 55th China Postdoctoral Science Foundation under project 2014M550407. L.N.Y. Wong acknowledges the support by the Singapore Academic Research Fund Tier 1 Grant (RG112/14), and the State Key Laboratory for GeoMechanics and Deep Underground Engineering, China University of Mining and Technology (SKLGDUEK1301). Several direct shear tests were performed by Z.C. Tang (supported by the Natural Science Foundation of China under project 40972178) at the Tongji University during the period of studying for his Ph.D. degree and thanks are given to Prof. Caichu Xia. Z.C. Tang wishes to thank Mr. Yinglong Song for preparing some of the specimens and assisting in the direct shear tests and Mr. Shantong Yang for preparing Fig 5.

## References

- Barton N (1973) Review of a new shear-strength criterion for rock joints. *Eng Geol* 7(4):287–332
- Barton N, Choubey V (1977) The shear strength of rock joint in theory and practice. *Rock Mech* 10(1):1–54
- Beer AJ, Stead D, Coggan JS (2002) Estimation of the joint roughness coefficient (JRC) by visual comparison. *Rock Mech Rock Eng* 35(1):65–74
- Grasselli G (2006) Shear strength of rock joints based on quantified surface description. *Rock Mech Rock Eng* 39(4):295–314
- Homand F, Belem T, Souley M (2001) Friction and degradation of rock joint surfaces under shear loads. *Int J Numer Anal Meth Geomech* 25(10):973–999
- Hong ES, Lee JS, Lee IM (2008) Underestimation of roughness in rough rock joints. *Int J Numer Anal Meth Geomech* 32(11):1385–1403
- ISRM (1978) Suggested methods for the quantitative description of discontinuities in rock masses. *Int J Rock Mech Min Sci Geomech Abstr* 15(6):319–368
- Kulatilake PHSW, Shou G, Huang TH, Morgan RM (1995) New peak shear strength criteria for anisotropic rock joints. *Int J Rock Mech Min Sci Geomech Abstr* 32(7):673–697
- Oh J, Kim GW (2010) Effect of opening on the shear behavior of a rock joint. *Bull Eng Geol Environ* 69(3):389–395
- Patton FD (1966) Multiple modes of shear failure in rock. In: *Proceedings of the 1st congress of the International Society for Rock Mechanics*, vol. 1, Lisbon, pp 509–513
- Tang ZC (2013) Mechanical behaviors of rock joint under different contact state and columnar jointed rock mass. Ph.D. thesis. Tongji University, Shanghai: (in Chinese with English abstract)
- Tang ZC, Liu QS, Xia CC, Song YL, Huang JH, Wang CB (2014) Mechanical model for predicting closure behavior of rock joints under normal stress. *Rock Mech Rock Eng* 47(6):2287–2298
- Tatone BSA, Grasselli G (2009) A method to evaluate the three-dimensional roughness of fracture surfaces in brittle geomaterials. *Rev Sci Instrum* 80(12):125110
- Xia CC, Tang ZC, Xiao WM, Song YL (2014) New peak shear strength criterion of rock joints based on quantified surface description. *Rock Mech Rock Eng* 47(2):387–400
- Yang J, Rong G, Cheng L, Hou D, Wang XJ (2015) Experimental study on peak shear strength criterion for rock joints. *Chin J Rock Mech Eng*. doi:10.13722/j.cnki.jrme.2014.1096 (in Chinese with English abstract)
- Zhao J (1997a) Joint surface matching and shear strength part B: JRC-JMC shear strength criterion. *Int J Rock Mech Min Sci* 34(2):179–185
- Zhao J (1997b) Joint surface matching and shear strength part A: joint matching coefficient (JMC). *Int J Rock Mech Min Sci* 34(2):173–178